# ECE imaging of electron temperature and electron temperature fluctuations (invited)

B. H. Deng, C. W. Domier, and N. C. Luhmann, Jr.[a)]
*Department of Applied Science, University of California at Davis, Davis, California 95616*

D. L. Brower
*Electrical Engineering Department, University of California at Los Angeles, Los Angeles, California 90095*

G. Cima
*Fusion Research Center, University of Texas and Austin, Austin, Texas 78712-1068*

A. J. H. Donné, T. Oyevaar, and M. J. van de Pol
*FOM-Inst. voor Plasmafysica Rijnhuizen, Association Euratom-FOM, Partner in the Trilateral Euregio Cluster, 3430 BE Nieuwegein, The Netherlands*

(Presented on 19 June 2000)

Electron cyclotron emission imaging (ECE imaging or ECEI) is a novel plasma diagnostic technique for the study of electron temperature profiles and fluctuations in magnetic fusion plasma devices. Instead of a single receiver located in the tokamak midplane as in conventional ECE radiometers, ECEI systems utilize large diameter imaging optics coupled with planar millimeter-wave imaging arrays to form multichannel ECE diagnostics with excellent spatial resolution. Combined with specially designed imaging optics, the use of these compact, low cost arrays has resulted in the excellent spatial resolution of the ECEI systems, the unique capability of two-dimensional measurements, and flexibility in the measurement of plasma fluctuations. Technical details and principles of this emerging diagnostic technique are described in this article. Illustrative experimental results are presented, together with a discussion of the further development of the diagnostic. © *2001 American Institute of Physics.* [DOI: 10.1063/1.1319864]

## I. INTRODUCTION

Electron cyclotron emission (ECE) radiometers have been standard tokamak diagnostics for measuring plasma electron temperature profiles since 1974,[1] and plasma electron temperature fluctuations since 1993.[2–4] The diagnostic is based on the facts that, in optically thick plasmas, the ECE intensity received by an antenna is proportional to the plasma electron temperature and that the ECE frequency in a tokamak is proportional to the magnetic field, which is a monotonically decreasing function of major radius. Thus, local $T_e$ values can be obtained by frequency resolved ECE radiometers. The measurement of $T_e$ fluctuations, however, had not been successful until intensity interferometric techniques were applied to ECE radiometers to reduce the intrinsic intensity fluctuation or radiation noise of ECE radiation,[2–4] which is usually significantly larger than that due to plasma instabilities.

Conventional ECE diagnostics measure electron temperature profiles by using a single antenna/receiver aligned along a horizontal chord in the direction of the major radius. Therefore, two-dimensional (2D) measurements are impossible with this single sight line arrangement. The spatial resolution of such a system in the transverse direction of the sight line is also limited due to the divergence of the far field beam pattern of the antenna; typically about 2–6 cm for small to medium size tokamaks.[5] Thus, conventional ECE radiometers cannot resolve fine scale structures (~1 cm) in $T_e$ profiles, or plasma fluctuations with a poloidal wave number $k > 1.5\,\mathrm{cm}^{-1}$ due to the sample volume effects.[6]

Recently, a novel ECE radiometer, the ECE Imaging or ECEI diagnostic, has been developed and applied to the TEXT-U, Rijnhuizen Tokamak Project (RTP), and TEXTOR tokamaks.[4,7,8] These diagnostic systems have high spatial resolution (~1 cm) and 2D measurement capability, and have demonstrated their power in the study of plasma fluctuations and transport.[4,7–10] In the following, the principle of this emerging diagnostic technique as well as ECEI system design details will be reviewed in Sec. II; illustrative experimental results will be presented in Sec. III; and the current development of the diagnostic will be presented in Sec. IV.

## II. ECE IMAGING DIAGNOSTIC SYSTEMS

### A. Principle of ECE imaging diagnostics

The principle of the diagnostic is illustrated in Fig. 1. Instead of a single receiver located in the tokamak midplane as in conventional ECE radiometers, the ECEI systems utilized newly developed millimeter-wave imaging arrays as the receiver/mixers. The elements of the arrays are aligned vertically, and measure at the same frequency, so that the sample volumes of the imaging systems are vertically aligned in the plasma. The horizontal position of the sample volumes are determined by the magnetic field strength and the frequency of ECE to be measured, which is essentially the local oscillator (LO) frequency for double side band re-

[a)]Electronic mail: ncluhmann@ucdavis.edu

 

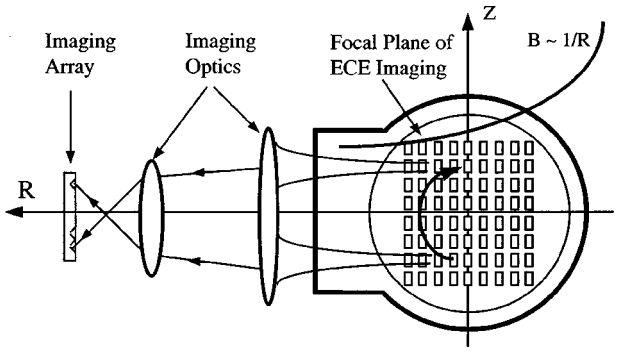


FIG. 1. Schematic of the ECEI diagnostic, showing the imaging array and the imaging lenses. The sample volumes of ECEI can be scanned horizontally to obtain 2D measurements.

ceivers. By varying the magnetic field strength or the LO frequency, the sample volumes can be scanned through the plasma minor cross section to achieve 2D measurements. As all the sample volumes are positioned at the focal plane of the imaging optics, i.e., the Gaussian beam waist location, excellent spatial resolution of about 1 cm (diameter at $1/e$ power) is achieved. With such improved spatial resolution, ECEI can resolve the small scale structures of the plasma electron temperature profiles, which were frequently observed in tokamaks with high power local heating.

One of the important issues for plasma fluctuation measurements is the sensitive poloidal wave number range due to the sample volume effects.[6] As the ECEI diagnostic has improved spatial resolution over that of conventional ECE systems, it is sensitive to fluctuations with $k<2.8\,\mathrm{cm}^{-1}$.[6] Figure 2 compares the sample volumes and sensitive $k$ ranges of several typical fluctuation diagnostics. Theoretical studies show that electrostatic fluctuations usually peak at $k_\perp \rho_i \sim 0.2-0.3$,[11] and for the plasmas of the TEXT-U, RTP, and TEXTOR tokamaks, the ion Larmor radius ($\rho_i$) is around 0.1–0.3 cm; thus, fluctuations peaking at $k\sim 1-3\,\mathrm{cm}^{-1}$ are expected. Therefore, ECEI is an ideal tool for the study of electrostatic fluctuations. Note too that the ECEI sample volumes can be separated both poloidally and radially (see Fig. 1); hence, it is possible to resolve the spectral asymmetry of the fluctuations in the wave number space.

### B. Imaging array

An ECE imaging system is comprised of an imaging array, imaging optics, a local oscillator source and power

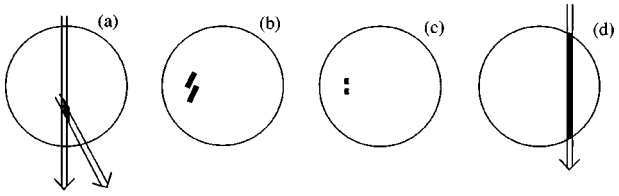


FIG. 2. Different fluctuation diagnostics have different sensitive wave number ranges due to sample volume effects. The far infrared (FIR) scattering is sensitive to $2<k<12\,\mathrm{cm}^{-1}$, the heavy ion beam probe is sensitive to $k<1.5\,\mathrm{cm}^{-1}$, the phase contrast imaging is sensitive to $0.4<k<12.9\,\mathrm{cm}^{-1}$, while ECE imaging is sensitive to $k<2.8\,\mathrm{cm}^{-1}$.

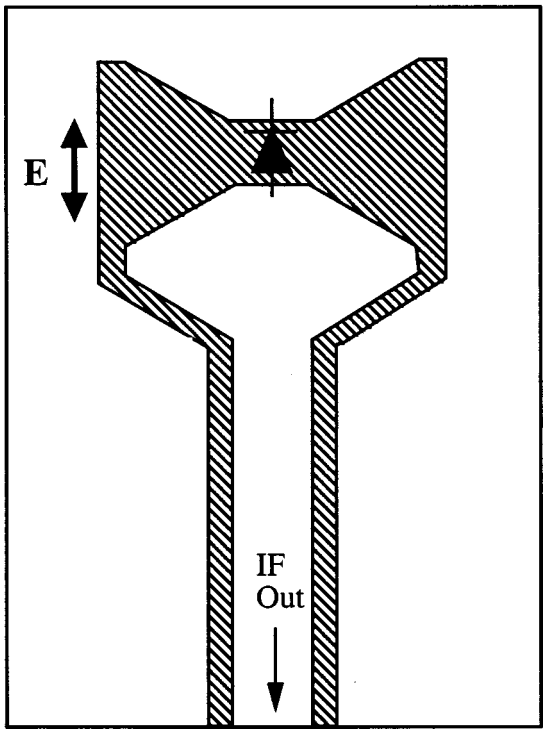


FIG. 3. The imaging array element is comprised of a SBT antenna and a Schottky barrier mixer diode.

coupling lenses, a mechanical support frame, and a signal detection system,[4] with the first two being the key components. The mixer/receiver arrays are comprised of planar slot bow tie (SBT) antennas integrated with beam-lead Schottky barrier diodes,[12] as illustrated in Fig. 3. The slot bow tie antennas were chosen as array elements as they offer wide radio frequency and intermediate frequency bandwidths, very small interchannel cross talk, ease of fabrication, and low cost.[4,12] Shown in Fig. 4 is a photograph of a hybrid imaging array fabricated on a printed circuit board and placed within an electrical shielding box. The LO power is transformed into an elliptical beam by lenses, usually one spherical, one cylindrical, to cover the entire array element.

There is currently no existing theoretical model that can be used to predict the sensitivity, radiation pattern, and bandwidth of the SBT antenna, and the theoretical and computer

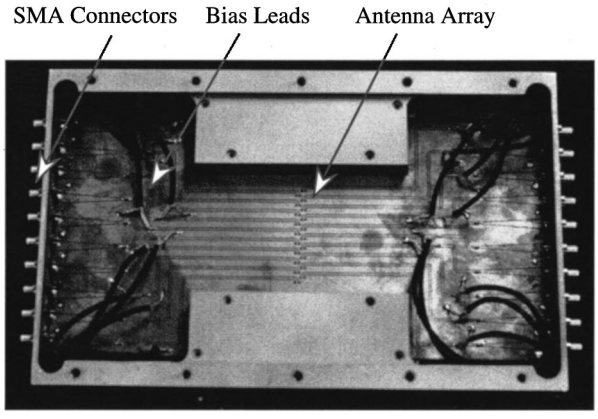


FIG. 4. A photo of the ECE imaging array within the shielding box.

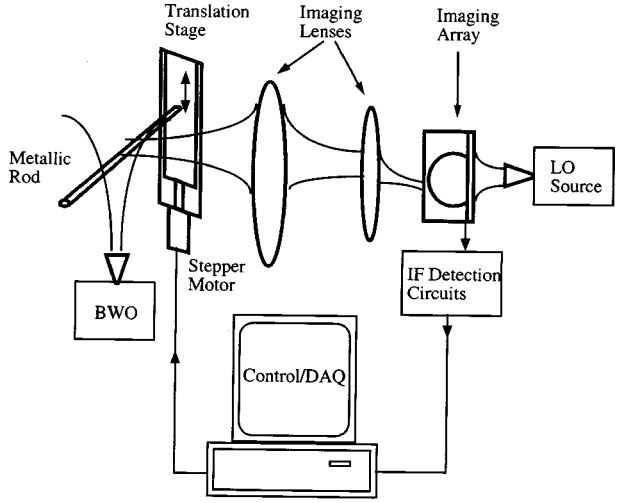


FIG. 5. Experimental arrangement for testing the channel spacing and focal plane spot sizes of the ECEI system.

design of the antenna is a current research project within the University of California, Davis group.[4] For the ECEI systems discussed in this article, the parameters of the antenna were chosen from tested model antennas, based on the system design requirements of frequency bands, radiation patterns, and spatial resolution.[4]

### C. Imaging optics

The imaging optics are comprised of large HDPE lenses, as shown in Fig. 1. Ray tracing codes were compiled to provide a one to one relation between the array elements and their images by choosing appropriate lens positions and focal lengths, to design the lenses, and to calculate the focal plane spot sizes using formulas of Gaussian beam propagation.[4] The goal of the optical design is to achieve the highest possible spatial resolution, consistent with constraints such as available port access, reasonable lens sizes, and lens fabrication cost. Generally, high spatial resolution requires that the focal plane spot size and the channel spacing be as small as possible. Given the optical magnification, which determines the channel spacing, a wider *E*-plane antenna pattern yields a smaller beam spot size. However, a smaller spot size results

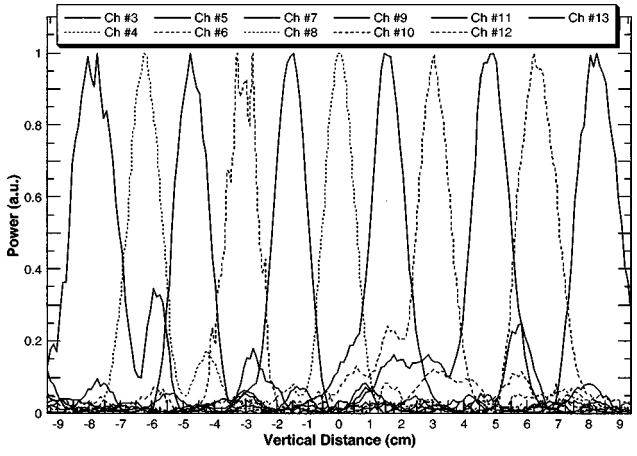


FIG. 6. Focal plane beam patterns of the TEXTOR ECEI system.

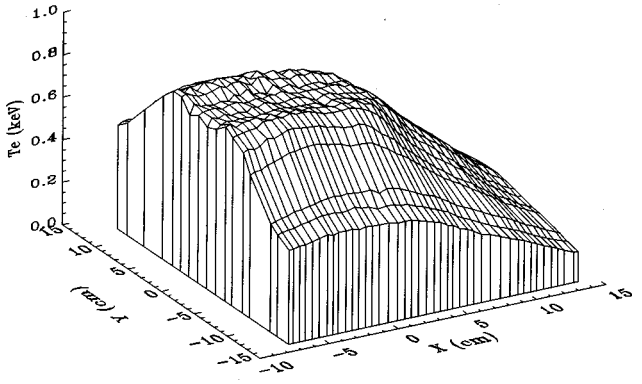


FIG. 7. 2D $T_e$ profile measured in the TEXT-U tokamak over the poloidal cross section.

in more rapid beam divergence, and hence larger beam size at the window, which can result in deleterious diffraction patterns. It is found that the port size and the distance between the plasma and the first imaging lens, which is determined by the access condition of the tokamak environment, are the main limiting factors for the achievable spatial resolution and coverage range of the plasma.

Prior to tokamak plasma experimental measurements, the system performance was determined in laboratory tests as shown in Fig. 5. In the testing, millimeter waves scattered from an aluminum rod form a line source which simulates the plasma ECE radiation, and the beam patterns of each channel were obtained by vertically translating the rod. The focal plane location of the imaging optics was determined by translating the system to obtain the narrowest beam patterns. Shown in Fig. 6 are the measured focal plane beam patterns of the TEXTOR ECEI system. The interchannel spacing is about 13 mm. The beam waist (diameter at $1/e$ intensity) is about 10 mm for the middle channels, and increases to about 18 mm for the edge channels due to spherical aberrations and edge diffraction, mainly due to limited port size. These parameters are close to that of both the TEXT-U and RTP systems.[4,7,8]

Beam refraction in the plasma will change the beam path for off-axis channels, and will change the Gaussian beam

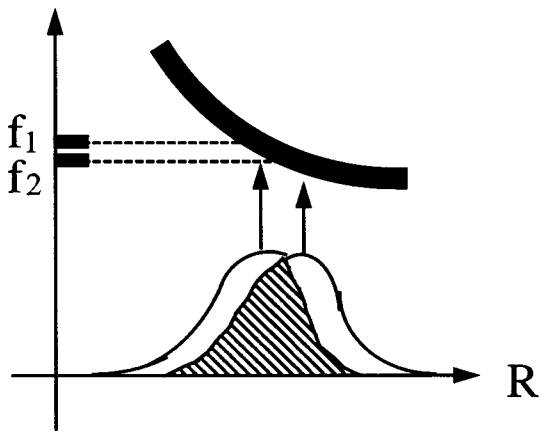


FIG. 8. Due to finite line width of ECE radiation, two signals measured with closely spaced, nonoverlapped frequency bands centered at $f_1$ and $f_2$ correspond to mostly overlapped sample volumes, and have uncorrelated radiation noises.

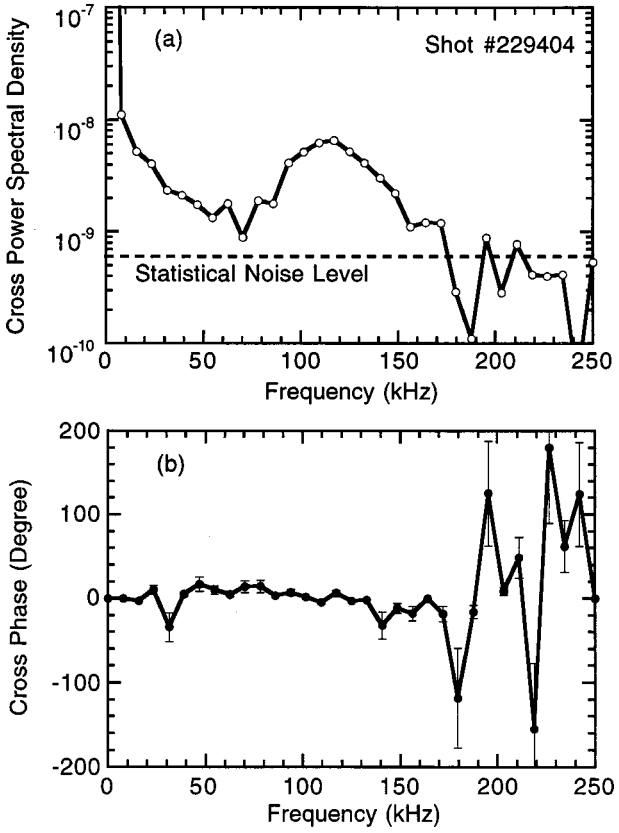


FIG. 9. Cross power spectral density of local $T_e$ fluctuations measured at 16 cm to the low field side of the plasma center. The data are from shot No. 229404 in TEXT-U with $I_p=150$ kA, $\bar{n}_e=2\times10^{19}$ m$^{-3}$, and $B_{\text{tot}}=2$ T.

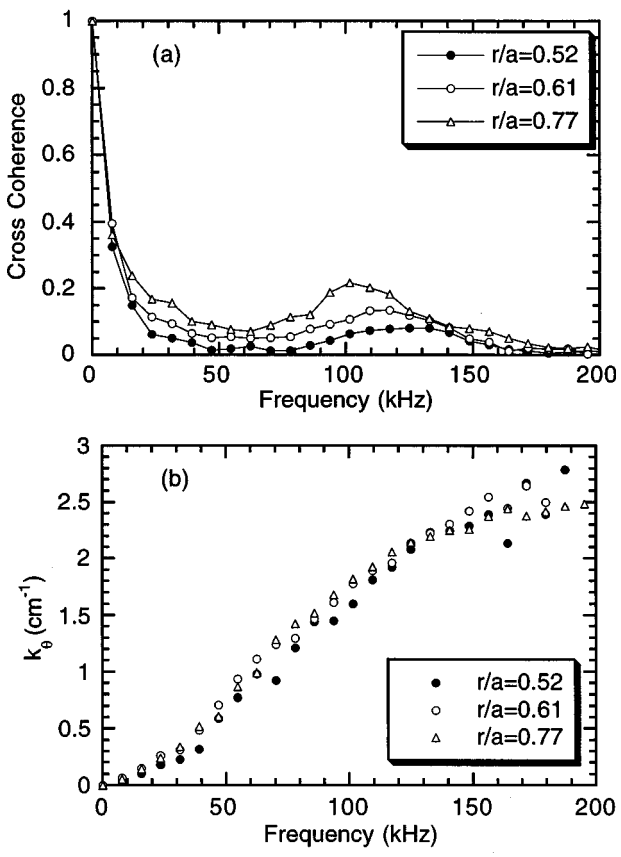


FIG. 10. Cross coherence function (a) and statistical dispersion relations (b) measured in TEXT-U ohmic plasmas by the same ECEI channel pair at different plasma radii. The plasma conditions are the same as that indicated in Fig. 9.

waist location, which could result in a slight increase in the beam spot size at resonance.[7] Recent simulations show that, in high density plasmas, especially in the high field side, these effects can be quite significant. In the experiments in RTP, the system position is adjusted before each discharge, based on the expected plasma density and associated focal plane shift, so that the degradation in spatial resolution is minimized. However, the change of the off-axis beam path needs to be corrected afterwards as necessary.

The side lobes shown in Fig. 6 are primarily due to edge diffraction. This could give rise to interchannel crosstalk, and thus limit the system resolution of fluctuation measurements. This can be partly minimized by making large lenses. However, as the port size is fixed, the spot size is chosen as a tradeoff between the spatial resolution and sidelobe levels. In Fig. 6, the worst case is the crosstalk between channel 3 and channel 4, with a common power of about 4%. As $T_e$ is proportional to the ECE power, the resultant minimum cross coherence between the $T_e$ fluctuations of the two channels is 0.04. This value is significantly smaller than the coherence due to plasma instabilities, usually between 0.1 and 0.9, depending on the mode and plasma conditions.

The above estimate of minimum detectable cross coherence will be reduced due to two other factors. First, the above estimate assumes that the beam extends uniformly in the toroidal direction ($H$ plane). For all the ECEI systems implemented, the beams are elliptical and elongate in the $H$ plane, and the separation between adjacent channels in the $H$ plane is much better than that in the $E$ plane which reduces the radiation noise common to the two channels. Second, even if the ECE radiation originates from the same plasma volume, it will reach the two adjacent channels at a different angle ($\sim1°$ difference). This small angle will cause the intensity fluctuation to slightly decorrelate.[2] From our experience, a minimum cross coherence of 0.02 is achieved.

## III. EXPERIMENTAL RESULTS

### A. Measurements of $T_e$ profiles

There are two operation modes of the ECEI systems. If spatial and temporal resolutions are important for the measurements, such as in the study of magnetohydrodynamic (MHD) and high frequency microturbulence, the LO fre-

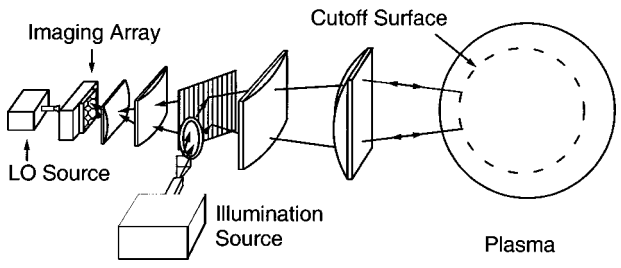


FIG. 11. Schematic of a microwave imaging reflectometer.

quency will be kept constant during the discharge, and the entire system will be translated to maintain a good focus when the resonance position is varied.[4,7,8] In the case of equilibrium profile measurements, the temporal resolution is not as critical, and the LO frequency can be swept during the discharge, so that the sample volumes are scanned across the plasma minor cross section to obtain a 2D profile. An example of this is shown in Fig. 7. It was measured in TEXT-U in an ohmic discharge (shot No. 227440, $I_p = 200\,\mathrm{kA}$, $\overline{n_e} = 1.6\times 10^{13}\,\mathrm{cm}^{-3}$, $B_t = 1.93\,\mathrm{T}$). It is seen that the temperature within the sawteeth inversion radius is quite uniform, which is typical of TEXT-U plasmas.[9] The calibration of the relative sensitivities is achieved by translating the plasma vertically and horizontally, and comparing the signals of adjacent channels corresponding to the same plasma volume.[4] The spatial resolution is about 1 cm horizontally, and about 1.3 cm vertically. Similar images are obtained every 0.8 ms during the discharge. Previously, 2D $T_e$ profiles were obtained in the Joint European Torus to verify that the magnetic flux surfaces are isothermal contours.[13]

In addition to measuring the equilibrium $T_e$ profiles, it is of great interest to monitor the magnetic island rotation over the plasma minor cross section. As shown previously by the authors,[4,8] ECEI diagnostics have the required excellent spatial resolution to resolve the island structures. Also, it is of particular importance is to measure the 2D $T_e$ profiles with a temporal resolution smaller than the period of the island rotation. This can be achieved by constructing a multichannel heterodyne receiver for each of the imaging channels, and is a goal of our future research.[4]

One of the difficulties for $T_e$ profile measurements is the sensitivity calibration. One way is to translate the plasma, as discussed above and in more detail in Ref. 4. Another convenient way is to compare the signals with the $T_e$ profiles measured by other diagnostics, such as Thomson scattering which was performed for the RTP and TEXTOR ECEI systems.[4,8,14] As the LO power is coupled to the imaging array quasioptically, the sensitivity is a strong function of LO frequency. Thus, it is necessary to calibrate the sensitivity when the LO frequency is varied or drifts.[4]

### B. Measurements of $T_e$ fluctuations

Intensity interferometric techniques are well established for measuring plasma $T_e$ fluctuations.[2–4,15] The ideal method adopted for ECEI systems is to decorrelate the radiation noise in the frequency domain.[3,4,15] This is possible due to the limited line width of ECE radiation, as illustrated in Fig. 8. An example of the measurement from an ohmic discharge in TEXT-U is shown in Fig. 9. The signals are from the same imaging receiver/mixer, and filtered by two different band pass filters.[4] The data are averaged over 250 ms so that the radiation noise power is less than that of the broadband drift wave turbulence [Fig. 9(a)].[4,10] The zero cross phases [Fig. 9(b)] verify that the signals are from the same plasma volume.

As ECE can be considered as blackbody radiation,[2] the correlation length of its intensity fluctuation is on the order of the electron Larmor radius, which is much smaller than the channel spacing of ECEI channels. Thus, signals from different ECEI channels have uncorrelated radiation noise, and therefore, we can apply the two point correlation technique to ECEI signals from different sample volumes to measure the wave number spectrum and statistical dispersion relations of $T_e$ fluctuations.[4,16] An example is shown in Fig. 10. It is seen that, at different plasma radii, the fluctuation amplitude and frequency varies due to different local $T_e$ gradients [Fig. 10(a)], while the phase velocities obtained from the statistical dispersion relations [Fig. 10(b)] are very similar due to the dominant $E\times B$ plasma rotation.[4,10] In Fig. 10(b), the turnover of the dispersion relations at $>170$ kHz is due to limited signal to noise ratio.[4]

## IV. FUTURE DEVELOPMENTS

One of the goals of future research is to construct fast 2D imaging systems to visualize the MHD island rotation over the plasma minor cross section, as discussed in Sec. III A. In addition, 2D imaging arrays are under development which will be utilized to construct 3D microwave imaging diagnostic systems for the study of plasma microturbulence.[4] These systems will combine the ECE imaging diagnostic and the reflectometric imaging diagnostic, so that both the electron temperature and density fluctuations as well as the correlation between these fluctuation quantities can be measured simultaneously. It is expected that new information obtained in this fashion will further advance the understanding of plasma microturbulence and related anomalous transport phenomena. As a first step, a microwave imaging reflectometry has been designed for TEXTOR, as shown in Fig. 11. A dichroic filter is utilized to separate the illumination wave from the reflection. As sampling in the image plane is equivalent to sampling in the plasma cutoff layer, it is expected that new data obtained in this fashion can be interpreted without the ambiguity in the interpretation of conventional reflectometry data due to wave scattering.[17]

## ACKNOWLEDGMENTS

This work is supported by the U.S. Department of Energy under Contract Nos. DE-FG03-95ER-54295 and W-7405-ENG-48, and by NWO and EURATOM.

[1] A. E. Costley, R. J. Hastie, J. W. M. Paul, and J. Chamberlian, Phys. Rev. Lett. **33**, 758 (1974).
[2] S. Sattler and H. J. Hartfuss, Plasma Phys. Controlled Fusion **35**, 1285 (1993).
[3] G. Cima, R. V. Bravenec, A. J. Wootton, T. D. Rempel, R. F. Gandy, C. Watts, and M. Kwon, Phys. Plasmas **2**, 720 (1995).
[4] B. H. Deng, Ph.D. dissertation, UC Davis (1999).
[5] H. J. Hartfuss, T. Geist, and M. Hirsch, Plasma Phys. Controlled Fusion **39**, 1693 (1997).
[6] R. V. Bravenec and A. J. Wootton, Rev. Sci. Instrum. **66**, 802 (1995).
[7] R. P. Hsia, B. H. Deng, W. R. Geck, C. Liang, C. W. Domier, N. C. Luhmann, Jr., D. L. Brower, and G. Cima, Rev. Sci. Instrum. **68**, 488 (1997).
[8] B. H. Deng, R. P. Hsia, C. W. Domier, S. R. Burns, T. R. Hillyer, N. C. Luhmann, Jr., T. Oyevaar, and A. J. H. Donné, Rev. Sci. Instrum. **70**, 998 (1999).

[9] G. Cima, K. W. Gentle, A. Wootton, D. L. Brower, L. Zeng, B. H. Deng, C. W. Domier, and N. C. Luhmann, Jr., Plasma Phys. Controlled Fusion **40**, 1149 (1998).
[10] B. H. Deng, D. L. Brower, G. Cima, C. W. Domier, N. C. Luhmann, Jr., and C. Watts, Phys. Plasmas **5**, 4117 (1998).
[11] P. C. Liewer, Nucl. Fusion **25**, 543 (1985).
[12] R. P. Hsia, Ph.D. dissertation, UC Davis (1998).
[13] D. V. Bartlett, D. J. Campbell, A. E. Costley, S. E. Kissel, S. Nowak, M. Brusati, and E. Lazzaro, Proceedings of the 14th European Conference on Controlled Fusion and Plasma Physics, Madrid, Spain, 1987, Vol. 11D, Part III, pp. 1252–1255.
[14] B. H. Deng, C. W. Domier, N. C. Luhmann, Jr., A. J. H. Donné, and M. J. van de Pol, Rev. Sci. Instrum. (these proceedings).
[15] H. J. Hartfuss and M. Hase, Proceedings of the Tenth Joint Workshop on Electron Cyclotron Emission and Electron Cyclotron Heating, Ameland, the Netherlands, 1997, p. 119.
[16] C. P. Ritz *et al.*, Rev. Sci. Instrum. **59**, 1739 (1988).
[17] E. Z. Mazzucato, Rev. Sci. Instrum. **69**, 2201 (1998).